NACA RM L56B01

NACA

RESEARCH MEMORANDUM

LOW-SPEED MEASUREMENTS OF STATIC STABILITY, DAMPING IN YAW, AND DAMPING IN ROLL OF A DELTA, A SWEPT, AND AN UNSWEPT WING FOR ANGLES OF ATTACK FROM 0° TO 90°

By Joseph L. Johnson, Jr.

Langley Aeronautical Laboratory
Langley Field, Va.

NATIONAL ADVISORY COMMITTEE FOR AERONAUTICS

WASHINGTON

April 13, 1956
Declassified February 26, 1958

NATIONAL ADVISORY COMMITTEE FOR AERONAUTICS

RESEARCH MEMORANDUM

LOW-SPEED MEASUREMENTS OF STATIC STABILITY, DAMPING IN YAW, AND DAMPING IN ROLL OF A DELTA, A SWEPT, AND AN UNSWEPT WING FOR ANGLES OF ATTACK FROM 0° TO 90°

By Joseph L. Johnson, Jr.

SUMMARY

A low-speed investigation has been conducted to determine the static longitudinal and lateral stability characteristics and the damping in yaw and damping in roll of a 60° delta wing, a 45° swept wing of aspect ratio 2.61, and an unswept wing of aspect ratio 3 over an angle-of-attack range from 0° to 90°.

The results of the investigation showed that the wings were longitudinally stable over the angle-of-attack range except for the delta wing which was about neutrally stable between 35° and 40° angle of attack. In general, the three wings were directionally stable below the stall but became directionally unstable at the stall and were about neutrally stable at high angles of attack. The effective dihedral was positive for the three wings over the angle-of-attack range except for the delta and swept wings near 30° angle of attack. In general, the damping in yaw about the body axis for the three wings was considerably smaller than that measured about the stability axis for the delta and swept wings at angles of attack near the stall. Very large values of damping in roll about the body axis were obtained for the delta and swept wings at angles of attack near the stall.

INTRODUCTION

An investigation is being conducted by the National Advisory Committee for Aeronautics to provide information on which preliminary studies of the stability and handling qualities of vertically rising airplane configurations can be based. The overall study consists of static force tests and oscillation tests to measure the stability and control characteristics

from 0° to 90° angle of attack of existing models of airplanes which are generally representative of possible vertically rising airplane configurations. The models tested previously have consisted of complete models and wing-fuselage combinations. (For example, see ref. 1.) The present investigation was undertaken to provide some basic information on the stability derivatives of wings alone from 0° to 90° angle of attack.

The investigation included static tests and free-to-damp oscillation tests from 0° to 90° angle of attack for a 60° delta wing, a 45° swept wing of aspect ratio 2.61, and an unswept wing of aspect ratio 3. Damping derivatives about the body axes were measured from 0° to 90° angle of attack and about the stability axes from 0° to 30° angle of attack. The effects of changes in the frequency or amplitude of the oscillation were not determined in this investigation.

SYMBOLS

Unless otherwise noted, all forces and moments are referred to the system of body axes originating at a center-of-gravity position of 25.0 percent of the mean aerodynamic chord and in the chord plane of the wings tested (see fig. 1). Ordinarily the subscript ω is used to denote derivatives obtained by oscillation techniques; however, since all the damping derivatives presented in this report were obtained from oscillation tests this subscript has been omitted for simplicity.

S	wing area, sq ft
$\bar{c}$	mean aerodynamic chord, ft, $\frac{2}{S}\int_0^{b/2} c^2 dy$
V	airspeed, ft/sec
q	dynamic pressure, lb/sq ft
ρ	air density, slug/cu ft
ψ	angle of yaw, deg
c	chord, ft
y	spanwise distance from plane of symmetry, ft
β	angle of sideslip (for the present tests $\beta = -\psi$), deg
ϕ	angle of roll, deg

α angle of attack, deg (In rolling or yawing oscillation tests about the body axes, the angle of attack varies with angle of bank or angle of yaw. The angles of attack specified in this report are the angles measured at zero bank and zero yaw.)

$\dot{\beta}$ rate of change of sideslip angle, rad/sec

r rate of change of yaw angle, rad/sec

p rate of change of roll angle, rad/sec

X longitudinal force, lb

Y lateral force, lb

Z force along Z-axis, lb

M pitching moment, lb-ft

N yawing moment, lb-ft

L rolling moment, lb-ft

C_X longitudinal force coefficient, X/qS

C_Z force coefficient along Z-axis, Z/qS

C_N normal-force coefficient $(-C_Z)$

C_m pitching-moment coefficient, $M/qS\bar{c}$

C_n yawing-moment coefficient, N/qSb

C_l rolling-moment coefficient, L/qSb

C_Y lateral-force coefficient, $\frac{Y}{qS}$

$C_{n_\beta} = \partial C_n/\partial\beta$, per deg

$C_{l_\beta} = \partial C_l/\partial\beta$, per deg

$C_{n_r} = \frac{\partial C_n}{\partial \frac{rb}{2V}}$, per radian

$C_{n_{\dot{\beta}}} = \frac{\partial C_n}{\partial \frac{\dot{\beta} b}{2V}}$, per radian

$C_{l_{\dot{\beta}}} = \frac{C_l}{\frac{\partial \dot{\beta} b}{2V}}$, per radian

$C_{l_p} = \frac{\partial C_l}{\frac{\partial pb}{2V}}$, per radian

k reduced-frequency parameter of the model, $\omega b/2V$

ω angular velocity, radians/sec

λ taper ratio; ratio of tip chord to root chord

Subscript:

s stability axes

APPARATUS AND MODELS

The static force tests and free-to-damp oscillation tests were conducted in the Langley free-flight tunnel. These tests were made using a sting-type support system and strain-gage balances. The apparatus used in this investigation was the same as that described in reference 1 for tests about the body axes. A drawing of this free-to-damp oscillation setup is shown in figure 2. The same test apparatus was also modified to allow free-to-damp oscillation tests about the stability axes. This modification, which is described in reference 2, consisted essentially of a circular track which was attached to the sting support to allow changes in the angle of attack of the model without changing the axis of rotation of the system.

The models used in this investigation were a 60° delta wing, a 45° sweptback wing of aspect ratio 2.61, and an unswept wing of aspect ratio 3. The delta wing had NACA 65-006.5 airfoil sections and both the swept and unswept wings had NACA 0012 airfoil sections. The three wing models used in this investigation were the same as those used in reference 3. The dimensional characteristics of these wings are given in table I.

TESTS

Force tests were made to determine the variations of C_N, C_X, and C_m over the angle-of-attack range from 0° to 90° for the three wings.

Values of C_Y, C_n, and C_l were measured for angles of sideslip of -20° to 20° over the angle-of-attack range.

Free-to-damp oscillation tests were made by the method described in reference 1 to determine the damping-in-yaw and damping-in-roll derivatives for the three wings from 0° to 90° angle of attack about the body axes and from 0° to 30° angle of attack about the stability axes.

The effects of changes in the frequency or amplitude of the oscillation on the damping derivatives were not determined in this investigation. All the oscillation tests about the body axes were made at a constant frequency for a given test setup. For the oscillation tests about the stability axes, the frequency varied with changes in angle of attack because of the type of equipment used. The frequencies at which the oscillation tests were made are shown in table II.

All tests were made at a dynamic pressure of about 4.72 pounds per square foot which corresponds to a velocity of about 64.5 feet per second and to a Reynolds number range from about 672,000 to 745,000 based on the mean aerodynamic chords of the wings tested.

For the oscillation tests the model was displaced in yaw or roll about 30° before being released and allowed to damp to 0° amplitude. The envelopes of the oscillations were plotted on semilogarithmic paper and were found to be fairly linear through the amplitude range investigated except for small amplitudes where the tunnel turbulence caused the data to be erratic. Because of the nonlinearity of the data at the small amplitudes, the logarithmic decrements or damping factors used to determine the damping derivatives were obtained generally from the slopes of the envelope curves for amplitudes above approximately ±2° and ±3°.

RESULTS AND DISCUSSION

Static Longitudinal Stability Characteristics

The longitudinal stability characteristics are presented in figure 3. The wings were longitudinally stable over the angle-of-attack range investigated except for the delta wing which was about neutrally stable between 35° and 40° angle of attack. These data generally show little change in stability with angle of attack except for the unswept wing near the stall. The unswept wing stalled at an angle of attack of about 16°, the swept wing at an angle of attack of about 25°, and the delta wing at an angle of attack of about 32°.

Static Lateral Stability Characteristics

The basic lateral stability data for the three wings are presented in figure 4. For the unswept wing, large displacements in the rolling- and yawing-moment curves are shown at 0° sideslip and at low angles of attack. The displacement from zero of the rolling-moment curves at 0° angles of attack and 0° sideslip is attributed primarily to asymmetry in the force test setup. The large displacements in these curves for the unswept wing at angles of attack from 14° to 16°, however, are attributed principally to unsymmetrical wing stalling.

The lateral stability parameters C_{n_β} and C_{l_β} which were determined from the data points of figure 4 for angles of sideslip of 5° and -5° are presented in figure 5. Since the basic data were erratic in some cases, particularly for the unswept wing near the stall, the curves shown in figure 5 were obtained by fairing through the points from figure 4. The data of figure 5 show that the wings were generally directionally stable below the stall except for the swept wing which had a slight amount of instability near 10° angle of attack. The wings became directionally unstable at the stall and were about neutrally stable at high angles of attack.

The effective dihedral of the delta wing and swept wing was positive $(-C_{l_\beta})$ over the angle-of-attack range except for angles of attack near 30°. The unswept wing had positive dihedral effect over the angle-of-attack range. A large increase in positive dihedral effect occurred for the unswept wing near the stall.

Damping Characteristics

Damping in yaw.- The values of the damping-in-yaw derivative $C_{n_r} - C_{n_{\dot\beta}} \cos \alpha$ and the damping-in-roll derivative $C_{l_p} + C_{l_{\dot\beta}} \sin \alpha$ measured relative to the body axes are presented in figures 6 and 7, respectively. Also presented in these figures are the damping-in-yaw and damping-in-roll derivatives measured about the stability axes from 0° to 30° angle of attack by the free-oscillation tests in this investigation. Values of $\left(C_{n_r} - C_{n_{\dot\beta}}\right)_s$ determined by forced-oscillation tests of reference 3 ($k = 0.08$) are presented in figure 6 for purposes of comparison.

The damping-in-yaw derivatives measured about the body axes show that the delta wing and swept wing had similar variations of this derivative over the angle-of-attack range. That is, both wings had positive damping (negative values of $C_{n_r} - C_{n_{\dot\beta}} \cos \alpha$) at low angles of attack and negative damping (positive values of $C_{n_r} - C_{n_{\dot\beta}} \cos \alpha$) at angles of

attack near 25°. At about 35° angle of attack these wings had their largest values of positive damping but a further increase in angle of attack reduced the damping in yaw and both wings had slightly negative damping in the higher angle-of-attack range. The unswept wing had positive damping in yaw over the angle-of-attack range except at the higher angles of attack. The largest value of positive damping occurred at an angle of attack of about 30° for the unswept wing.

The oscillation data measured in this investigation about the stability axis show large positive values of damping in yaw up to 30° angle of attack for the swept and delta wings. These free-to-damp oscillation data are in fairly good agreement with the forced-oscillation data from reference 3. In the case of the unswept wing, the values are relatively small at all angles of attack and the two sets of data are in fairly good agreement except near the stall.

Damping in roll.- The damping-in-roll derivatives measured about the body axes (fig. 7) indicate that the delta wing and swept wing had positive damping $\left(\text{negative values of } Cl_p + Cl_\beta \sin \alpha\right)$ over the angle-of-attack range with a large increase in damping near angles of attack of 30°. The unswept wing had positive damping at low angles of attack but had relatively large values of negative damping over the angle-of-attack range from about 17° to 67°.

The damping-in-roll data measured about the stability axes generally indicate a decrease in positive damping with increasing angle of attack for all three wings with the unswept wing becoming about neutrally stable near 20° angle of attack.

CONCLUDING REMARKS

The results of the low-speed investigation to determine the static and damping derivatives of a 60° delta wing, a 45° swept wing, and an unswept wing from 0° to 90° angle of attack may be summarized as follows:

1. The wings were longitudinally stable over the angle-of-attack range except for the delta wing which was about neutrally stable between 35° and 40° angle of attack.

2. In general, the three wings were directionally stable below the stall but became directionally unstable at the stall and were about neutrally stable at high angles of attack. The effective dihedral was positive for the three wings over the angle-of-attack range except for the delta and swept wings near 30° angle of attack.

3. The damping in yaw about the body axis for the three wings was considerably smaller than that measured about the stability axis for the delta and swept wings near the stall.

4. Very large values of damping in roll about the body axis were obtained for the delta and swept wings at angles of attack near the stall.

Langley Aeronautical Laboratory,
National Advisory Committee for Aeronautics,
Langley Field, Va., January 19, 1956.

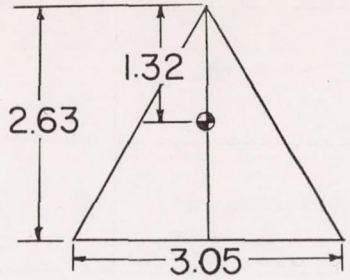
REFERENCES

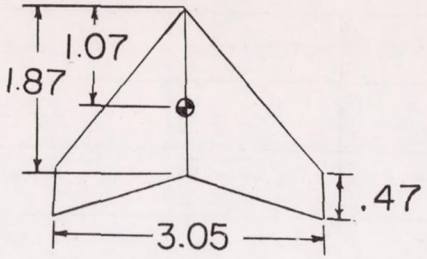
1. Hewes, Donald E.: Low-Speed Measurement of Static Stability and Damping Derivatives of a 60° Delta-Wing Model for Angles of Attack of 0° to 90°. NACA RM L54G22a, 1954.

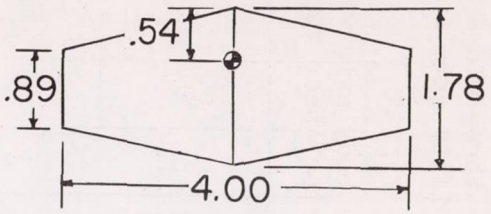
2. Johnson, Joseph L., Jr.: Low-Speed Measurements of Rolling and Yawing Stability Derivatives of a 60° Delta-Wing Model. NACA RM L54G27, 1954.

3. Campbell, John P., Johnson, Joseph L., Jr., and Hewes, Donald E.: Low-Speed Study of the Effect of Frequency on the Stability Derivatives of Wings Oscillating in Yaw With Particular Reference to High Angle-of-Attack Conditions. NACA RM L55H05, 1955.

Table I- Dimensional characteristics of the wings.
All dimensions in feet.







Type	Delta	Swept	Unswept
Sweep	60°(L.E.)	45° ($\bar{c}$/4)	0° ($\bar{c}$/2)
Area	4.05 sq ft	3.56 sq ft	5.35 sq ft
$\bar{c}$	1.76 ft	1.31 ft	1.38 ft
Aspect ratio	2.31	2.61	3.00
λ	0	.25	.50
Airfoil	NACA65-006.5	NACA 0012	NACA 0012

TABLE II

RANGE OF OSCILLATION TEST FREQUENCIES

Wing	Derivative	Axes	Frequency, cps		$\omega b/2V$	
			$\alpha = 0^\circ$	$\alpha = 30^\circ$	$\alpha = 0^\circ$	$\alpha = 30^\circ$
Delta	Damping in yaw	Body	0.81	0.81	0.120	0.120
		Stability	.89	.61	.134	.09
	Damping in roll	Body	.88	.88	.130	.130
		Stability	.95	.66	.142	.10
Swept	Damping in yaw	Body	.86	.86	.126	.126
		Stability	.92	.60	.136	.09
	Damping in roll	Body	.88	.88	.130	.130
		Stability	.90	.66	.135	.10
Unswept	Damping in yaw	Body	.87	.87	.169	.169
		Stability	.93	.60	.18	.117
	Damping in roll	Body	.87	.87	.169	.169
		Stability	1.00	.62	.19	.12

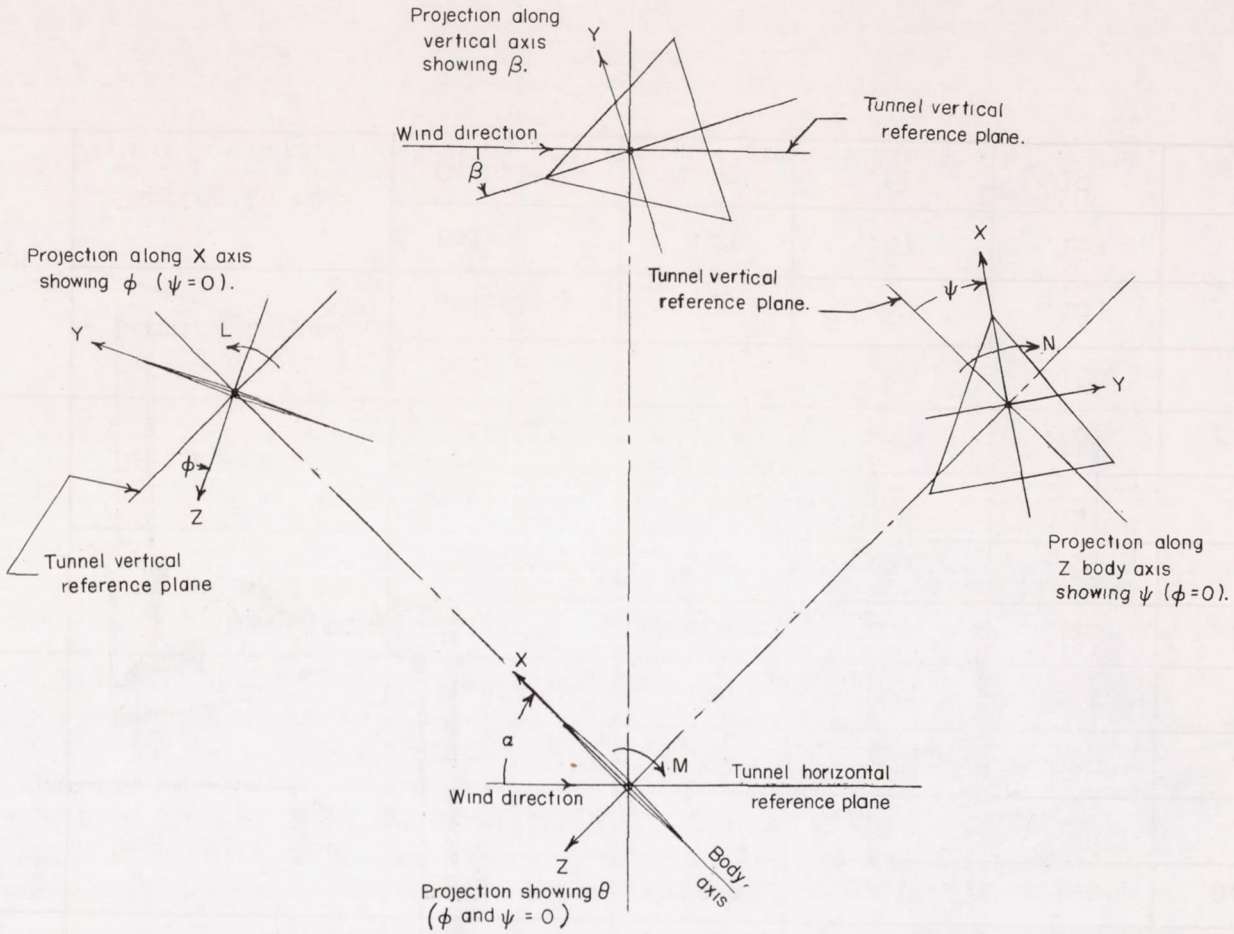
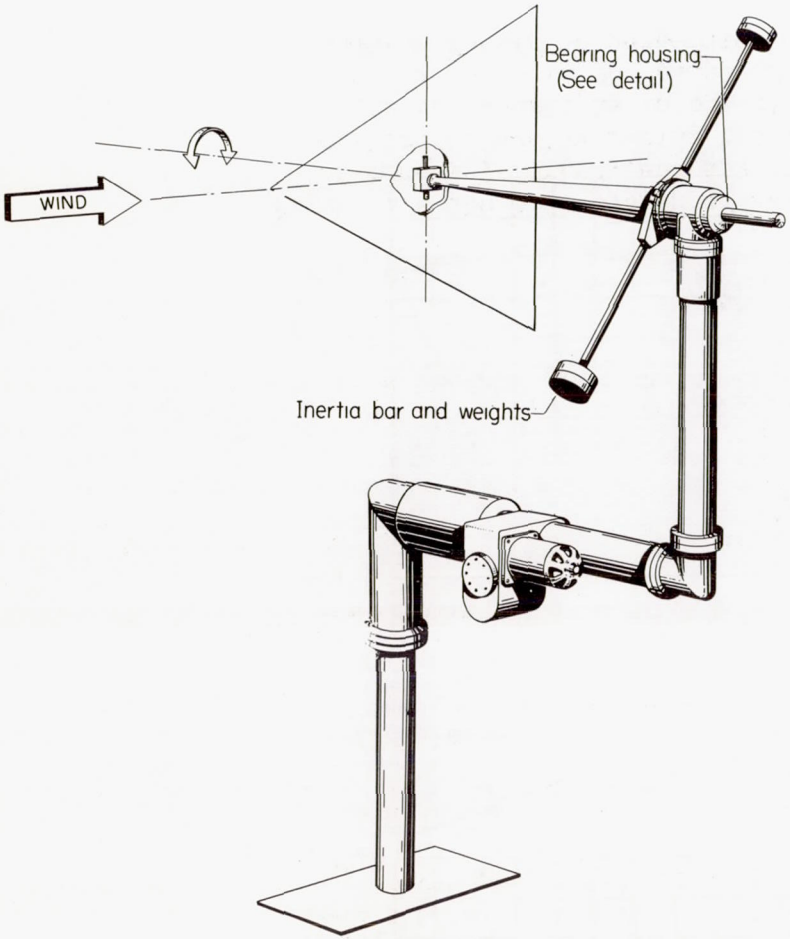
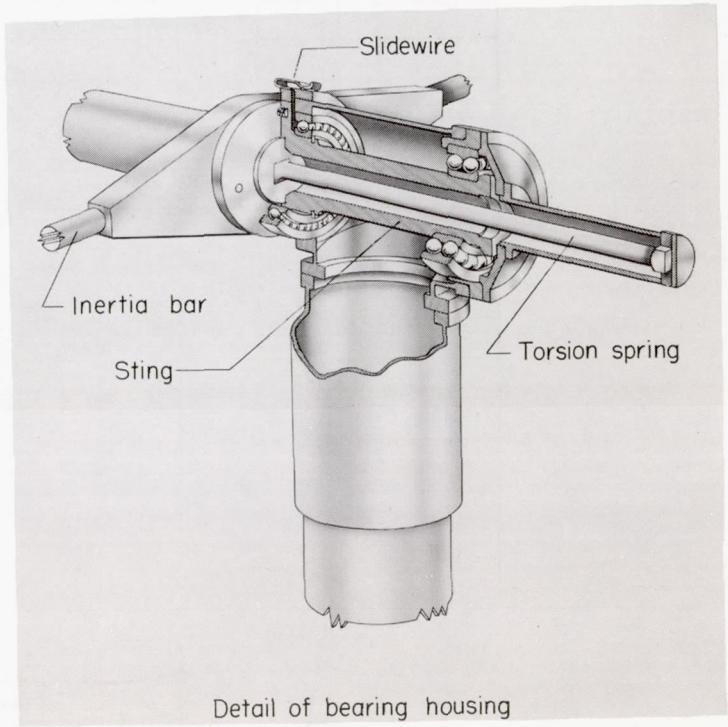


Figure 1.- The body system of axes. Arrows indicate positive directions of moments, forces, and angles. This system of axes is defined as an orthogonal system having the origin at the center of gravity and in which the X-axis is in the plane of symmetry and the wing chord plane, the Z-axis is in the plane of symmetry and perpendicular to the X-axis, and the Y-axis is perpendicular to the plane of symmetry.





L-89380

Figure 2.- Schematic drawings of free-to-damp oscillation apparatus.

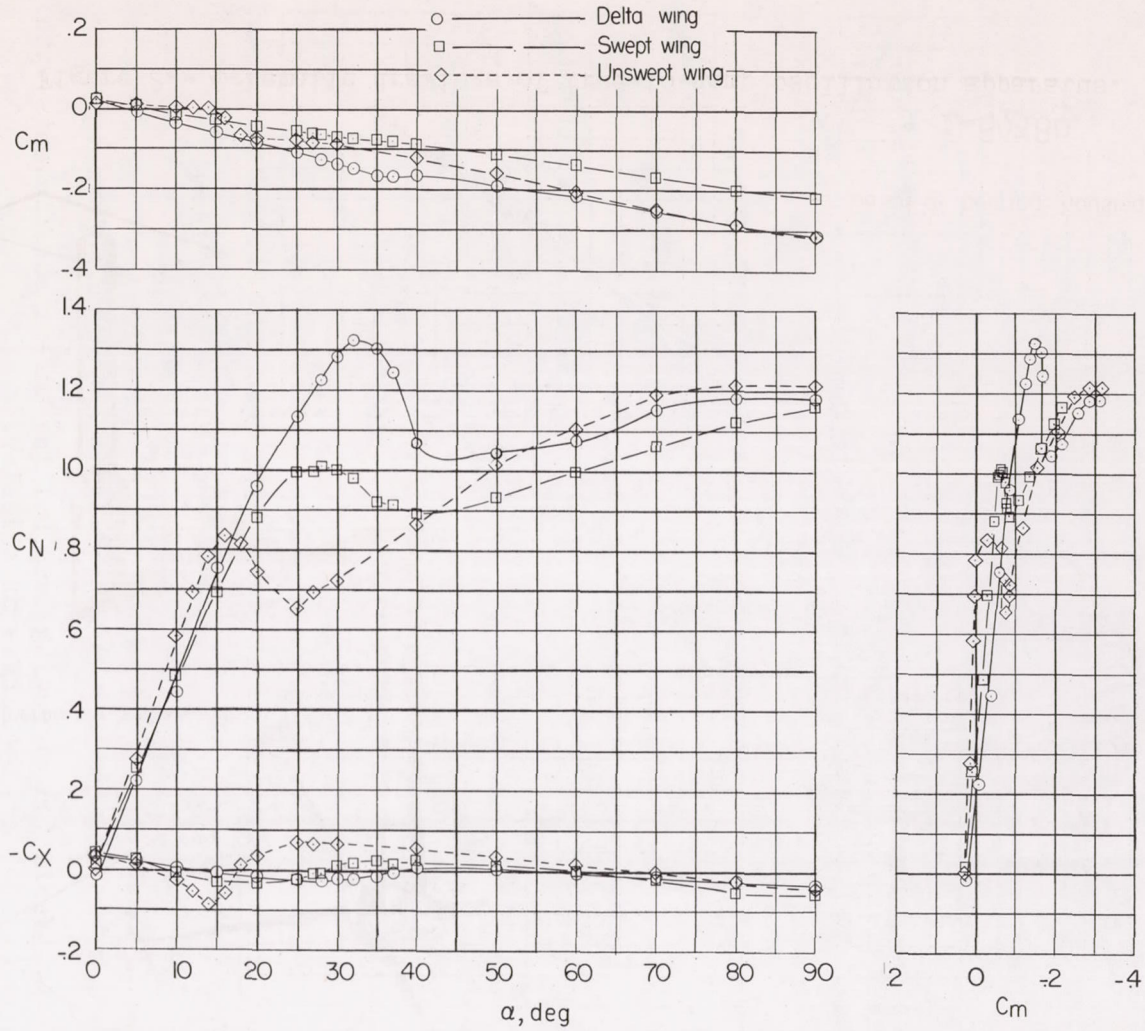
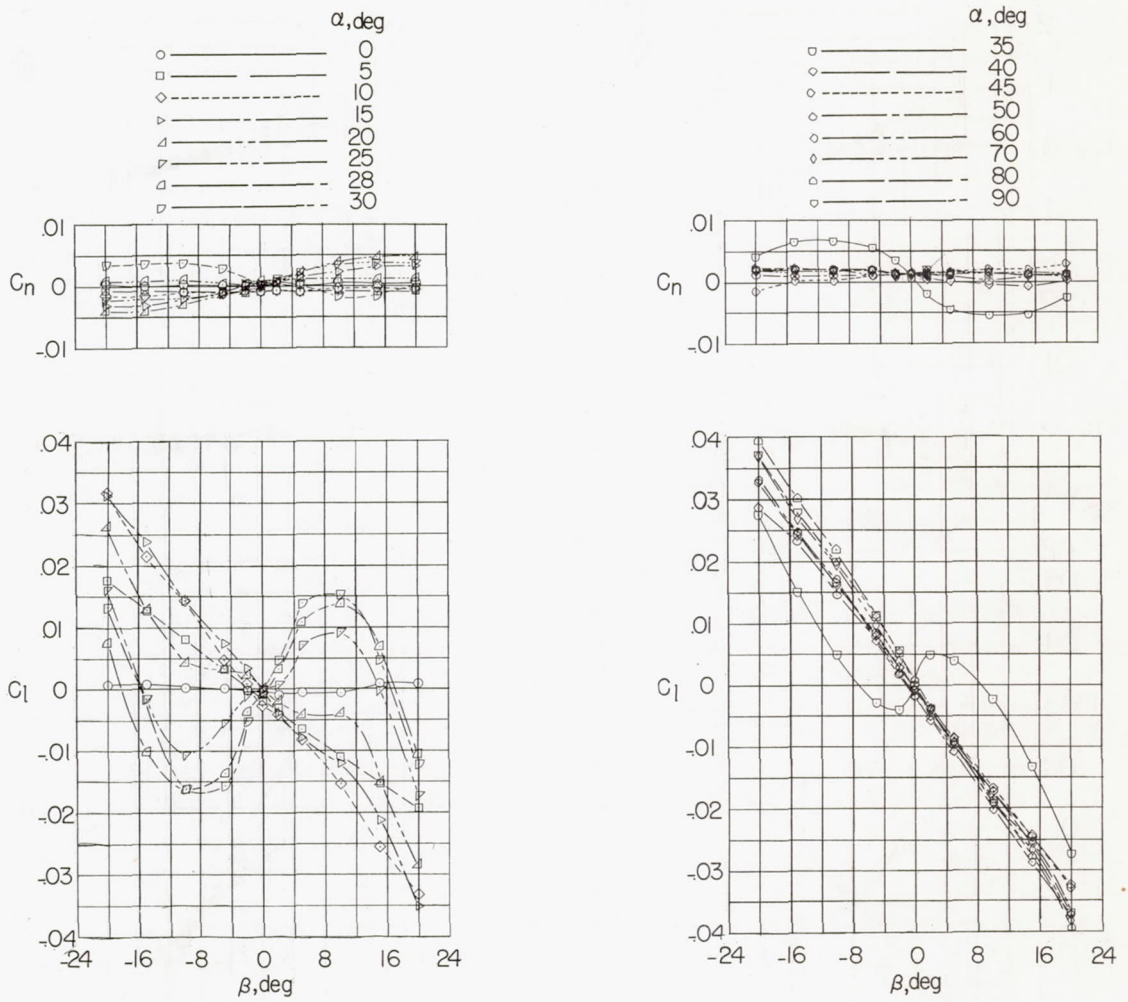
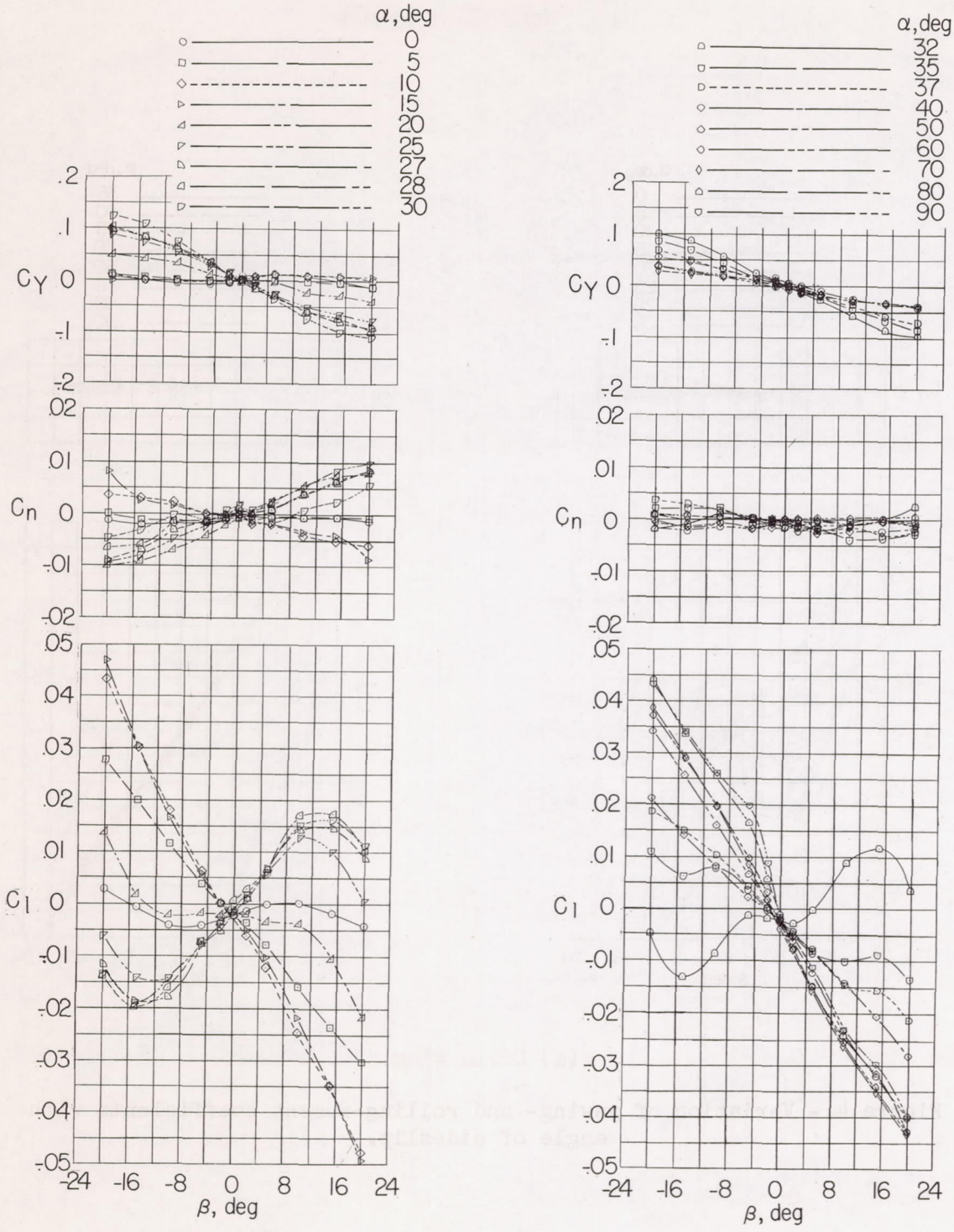


Figure 3.- Static longitudinal stability characteristics of the three wings.



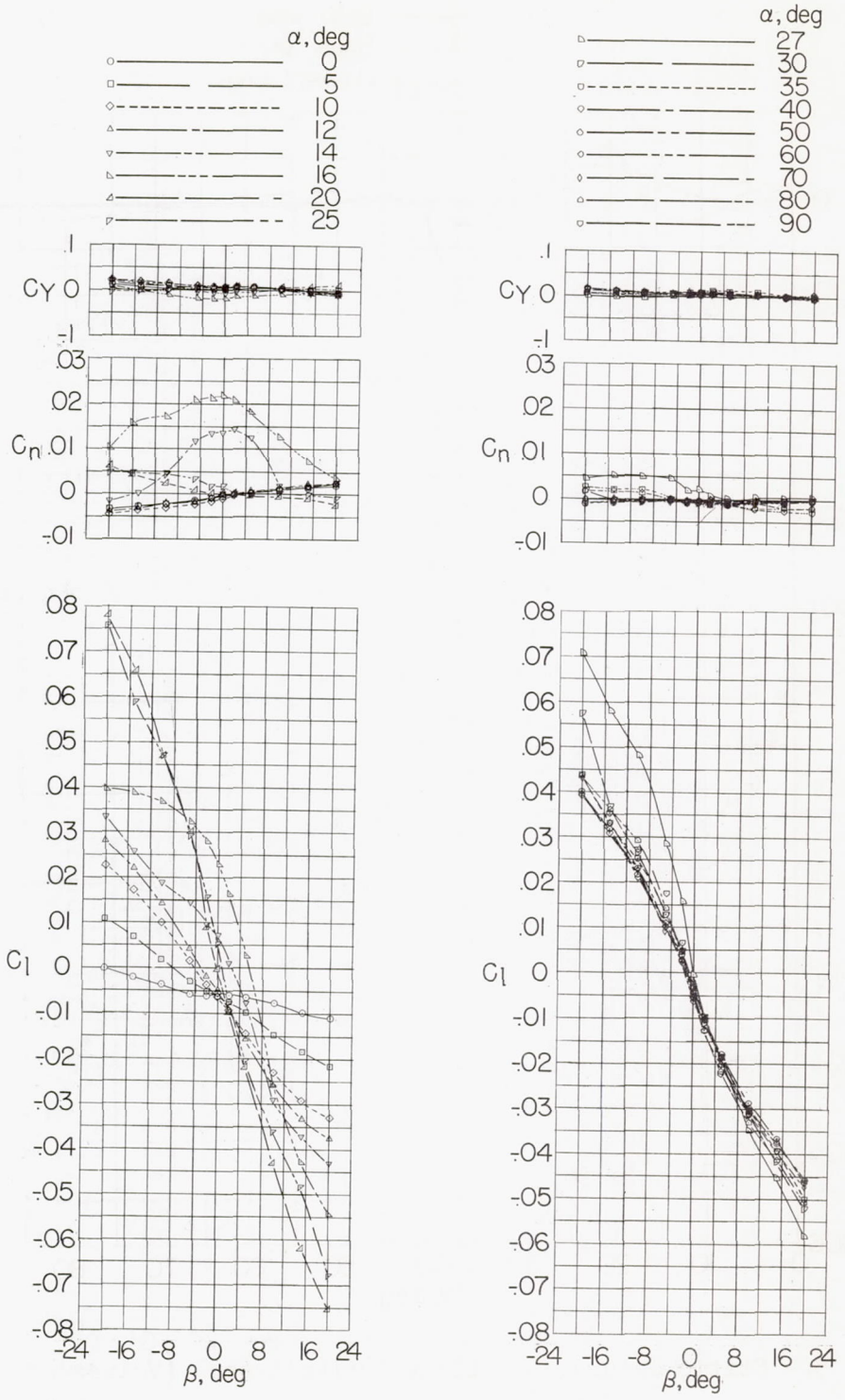
(a) Delta wing.

Figure 4.- Variation of yawing- and rolling-moment coefficients with angle of sideslip.



(b) Swept wing.

Figure 4.- Continued.



(c) Unswept wing.

Figure 4.- Concluded.

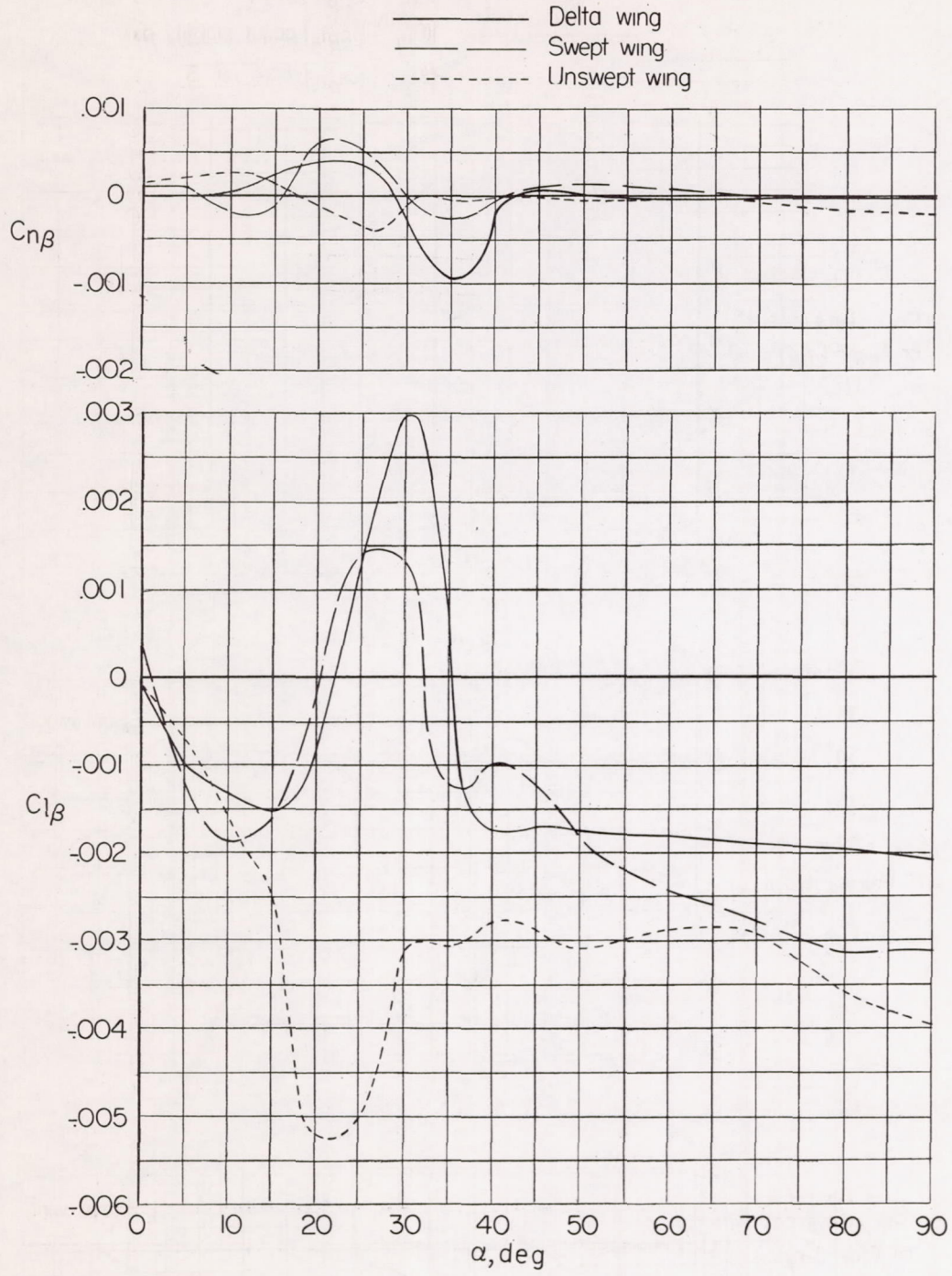


Figure 5.- Static lateral stability derivatives. (Values of C_{n_β} and C_{l_β} determined from data points between $\beta = 5^\circ$ and -5° of the curves of fig. 4.)

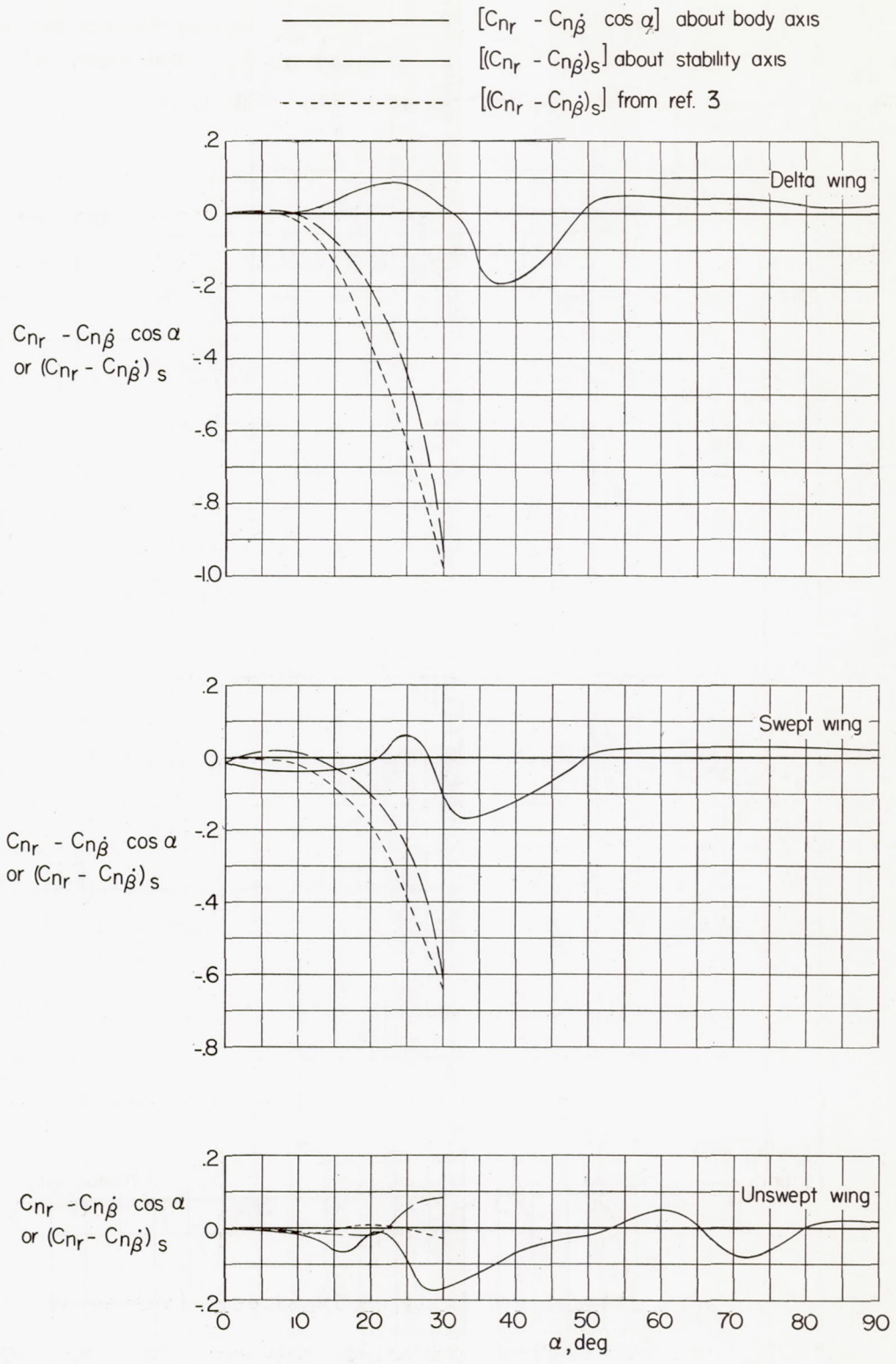


Figure 6.- Damping-in-yaw derivatives. (See table I for frequencies at which data were obtained. Reference 3 data presented for k = 0.08.)

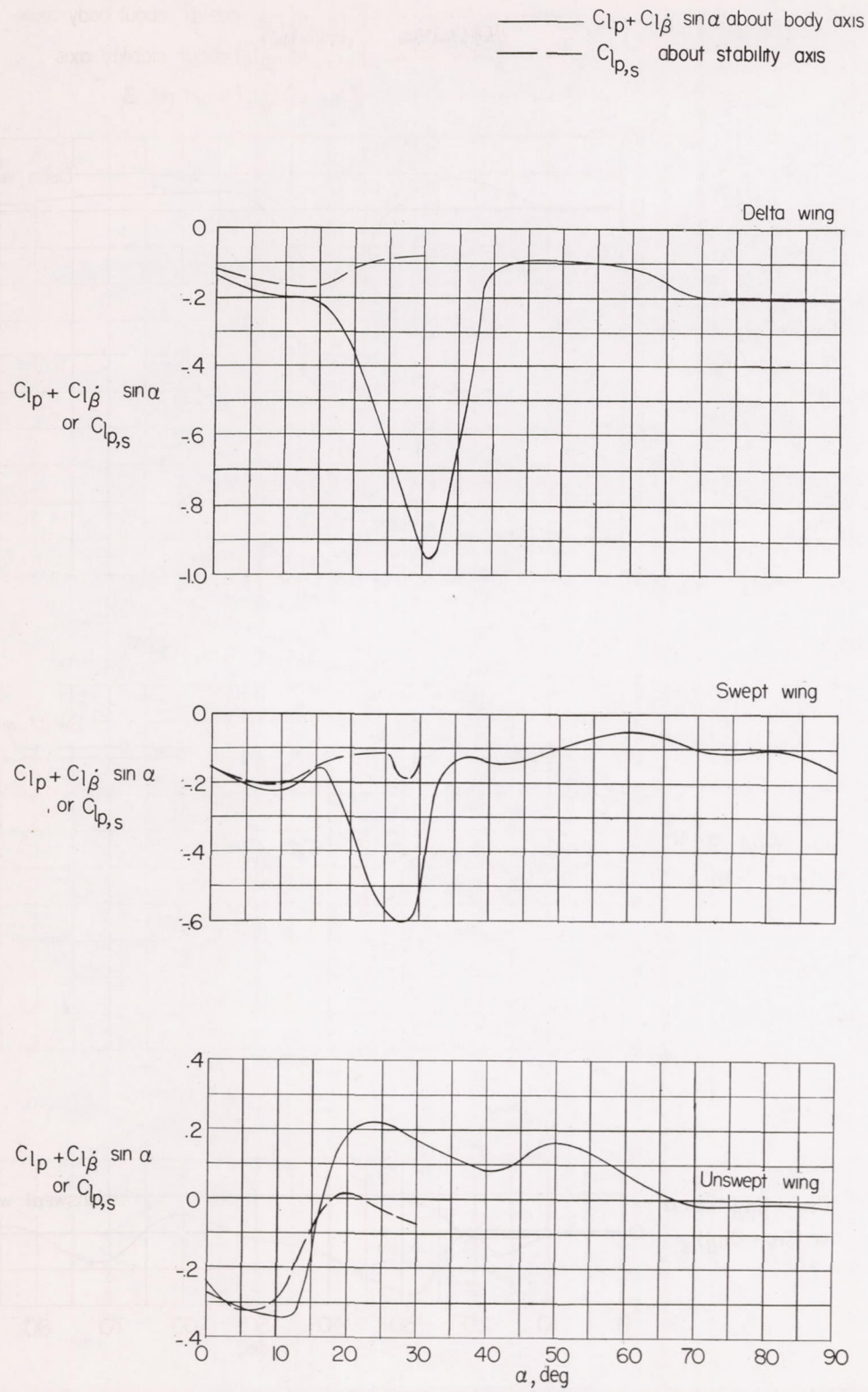


Figure 7.- Damping-in-roll derivatives.